POLITECNICO DI TORINO
Repository ISTITUZIONALE

Sound transmission properties of a porous meta-material with periodically embedded Helmholtz resonators

Original
Sound transmission properties of a porous meta-material with periodically embedded Helmholtz resonators / Magliacano, D., Catapane, G., Petrone, G., Verdière, K., Robin, O.. - In: MECHANICS OF ADVANCED MATERIALS AND STRUCTURES. - ISSN 1537-6494. - ELETTRONICO. - 31:25(2024), pp. 6748-6756. [10.1080/15376494.2023.2237699]

Availability:
This version is available at: 11583/2980565 since: 2025-02-04T11:18:28Z

Publisher:
Taylor & Francis Group, LLC

Published
DOI:10.1080/15376494.2023.2237699

Terms of use:

This article is made available under terms and conditions as specified in the corresponding bibliographic description in the repository

Publisher copyright
Taylor and Francis postprint/Author's Accepted Manuscript con licenza CC by-nc-nd

This is an Accepted Manuscript version of the following article: Sound transmission properties of a porous meta-material with periodically embedded Helmholtz resonators / Magliacano, D., Catapane, G., Petrone, G., Verdière, K., Robin, O.. - In: MECHANICS OF ADVANCED MATERIALS AND STRUCTURES. - ISSN 1537-6494. - ELETTRONICO. - 31:25(2024), pp. 6748-6756. [10.1080/15376494.2023.2237699]. It is deposited

(Article begins on next page)

19 November 2026

Sound transmission properties of a porous meta-material with periodically embedded Helmholtz resonators

Dario Magliacano[a,b,*], Giuseppe Catapane[c], Giuseppe Petrone[c,b], Kevin Verdière[d], Olivier Robin[e]

[a] *Department of Mechanical and Aerospace Engineering, Politecnico di Torino, Corso Duca degli Abruzzi 24, 10129 Turin, Italy*
[b] *WaveSet S.R.L., Via A. Gramsci 15, 80122 Naples, Italy*
[c] *PASTA-Lab (Laboratory for Promoting experiences in Aeronautical STructures and Acoustics), Department of Industrial Engineering - Aerospace Section, Università degli Studi di Napoli "Federico II", Via Claudio 21, 80125 Naples, Italy*
[d] *Mecanum Inc., 2444 Bonin, Sherbrooke (Québec) J1K 1C4, Canada*
[e] *Centre de Recherche Acoustique-Signal-Humain, Department of Mechanical Engineering, Université de Sherbrooke, 2500 boulevard de l'Université, Sherbrooke (Québec) J1K 2R1, Canada*

Abstract

The main scope of this work is to study the effect of embedding a periodic pattern inside a porous material, in order to passively improving its acoustic performance in terms of sound transmission loss. A contemplated application is the improvement of classical aeronautical soundproofing packages. In order to reach this goal, numerical models of an acoustic package including periodic patterns are implemented using the finite element method and the Transfer Matrix Method. Firstly, some of the proposed configurations are experimentally tested, providing a comparison and validation of the obtained numerical results. Afterwards, several configurations of inclusions are numerically studied, and incorporate hollow cylindrical inclusions, half-cut hollow cylindrical inclusions and cylindrical Helmholtz resonators. The improvements in terms of transmission loss, essentially brought by a periodicity peak, are evaluated under plane wave excitation with various incidence angles. The main novelties of the present work are represented by an experimental validation of

*Corresponding author
Email address: dario.magliacano@polito.it (Dario Magliacano)

the proposed acoustic meta-materials that were only numerically studied in previous works. The effect of the inclusion of a periodic pattern of Helmholtz resonators inside the foam core is also considered. The presented numerical results are also evaluated for different incidence angles of an exciting acoustic plane wave.

Keywords: acoustics, Sound Transmission Loss, meta-materials, foam, periodicity, Helmholtz resonator

---

Nomenclature

c_0	sound speed in air
d	dimension of the unit cell
d_{cavity}	main length of the cavity in the section plane
d_{neck}	main length of the neck in the section plane
E	Young modulus
f_{res}	resonance frequency
j	imaginary unit
$K = \rho(\frac{\omega}{k})^2$	bulk modulus
k	wave number
L	length of the tube
l_{eff}	effective length of the neck out of the section plane
m	odd-integer multiple of the wavelength quarter
n	number of unit cells along the thickness
r	outer radius of the inclusion
S_{neck}	area of the section of the neck
t	thickness of the inclusion
T	total thickness of the acoustic package
TL	Transmission Loss
V_{cavity}	volume of the cavity
x, y, z	space coordinates
$Z_c = \sqrt{K\rho}$	characteristic impedance
θ, ϕ	angles of incidence
$\lambda = \frac{2\pi}{k}$	wavelength
ν	Poisson coefficient
ξ	ratio between the neck/cavity lengths in the section plane
$\Pi_{incident}$	incident power
$\Pi_{transmitted}$	transmitted power
ρ	density
ρ_0	density of air
ω	angular frequency

1. Introduction

The importance of environmental noise control has increased with modern urbanization and transportation traffic and associated noise-induced health

impairments, such as irritation, sleep disruption, or even ischemic heart disease [1]. In this context, the transportation industry has to cope with several not-trivial compromises. For instance, an aircraft design procedure cannot neglect sound emission considerations and an aircraft will not be sold or certified if too noisy. Nevertheless, sound reduction systems or sound packages should be as lightweight as possible and installed in available spaces that are usually reduced.

Classical sound absorbing devices or materials may be classified into two different fields: acoustic resonators [2] and porous media. Acoustic resonators mainly include perforated panels [3] Helmholtz resonators (HRs) [4, 5] or quarter wavelength resonators [6] These solutions can reach large performance at low frequencies, but only on narrow frequency bands [7]. Porous media for acoustic purposes are materials that include channels, cracks or cavities within a rigid skeleton, which concretely let the sound waves enter the media and dissipate their energy by viscous and thermal losses; these energy consumption dynamics allow sound absorption over a large frequency range [8, 9]. Porous media lack efficiency at low frequencies, but reach large performance at medium and high frequencies [10]. This limitation can be overcome through the use of multi-layer configurations [11], but the improvement brought by these solutions is a function of the allowable thickness or total mass of a soundproofing configuration [12, 13].

Acoustic meta-materials were introduced to successfully overcome these limitations [14]. They offer great flexibility for manipulating sound waves and promise unprecedented functionality, ranging from transformation acoustics, super-resolution imaging to acoustic cloaking [15]. Meta-materials have several applications in several engineering field like energy, civil and transportation (aerospace, automotive, railway), for which a compromise between space, weight and acoustic comfort is needed [16, 17]. However, the design of acoustic meta-materials with exciting functionality remains challenging with traditional approaches using classic acoustic elements; thus, for some specific design and characterization applications, also innovative approaches based on machine-learning algorithms have been proposed in the literature [18, 19].

The concept of Helmholtz resonance and the associated classical theory have been applied in the design and analysis of various systems, including tuned intake manifolds of vehicles [20–22], noise attenuation in pipelines [23], attenuation of aircraft propeller noise [24], and combustion instabilities for gas-turbine engines [25]. Another interesting way to improve the efficiency of acoustic packages is constituted by the use of porous media with em-

bedded periodic inclusions [26, 27], which exhibit specific dynamic filtering effects. Their design is based on substructures that, if correctly shaped and arranged, allow improved sound absorption [28]; for instance, such a configuration may also be considered to enhance the acoustical behavior of the core of a sandwich-like structure [29, 30]. Several studies concerning the acoustic optimization of stiffened [31] and sandwich [32, 33] panels can be found in the literature [34, 35]. Also, the nature of a sandwich core may have a strong influence on the acoustic behavior of aerospace structures [36, 37], for both solid foams [38] and porous [39, 40] or poro-elastic [41–45] layers. In addition, it has been demonstrated that the core geometry plays a relevant role too [46].

The present work is structured as follows: in Section 2, used quantities (Sound Transmission Loss, abbreviated TL), systems (Helmholtz resonators) and calculation approaches are introduced. The AcuH toolbox developed by WaveSet S.R.L. [47] is used in order to perform calculations based on the Transfer Matrix Method (TMM) for multi-layered configurations. In Section 3, the materials used for the acoustic package and the geometrical properties of the analyzed configurations are detailed. In Section 4, some configurations are experimentally analyzed, leading to a comparison and validation of the obtained numerical results. In Section 5 the numerical results corresponding to the conducted calculations are reported and discussed. In particular, the effect of several periodic patterns (involving hollow cylindrical inclusions, half-cut hollow cylindrical inclusions and cylindrical Helmholtz resonators) is studied. For each of these layouts, the improvement in terms of sound transmission loss is evaluated. Moreover, in Section 6numerical results are evaluated for different angles of incidence of a plane wave exciting the system. In Section 7 some concluding considerations are developed, the main achievements of the present research are summarized and commented, and some possible future expansions are identified and evaluated.

2. Theoretical and methodological framework

2.1. Helmholtz resonators

A Helmholtz resonator (HR) is a tunable device whose geometry is usually represented by a neck followed by a cavity, its structure being made of walls considered rigid and filled with fluid. A HR is usually assimilated to a mass-spring system, in which the air volume acts as a spring, and the fluid in the

neck represents the mass. As a one degree-of-freedom system, it exhibits a single resonance frequency f_{res} defined as:

$$f_{res} = \frac{c_0}{2\pi}\sqrt{\frac{S_{neck}}{V_{cavity} l_{eff}}}, \tag{1}$$

where c_0 is the sound speed in air, S_{neck} is the area of the section of the neck, V_{cavity} is the volume of the cavity and l_{eff} is the effective length of the neck out of the section plane. The equations reported in this sub-section are theoretically valid for a Helmholtz resonator with perfectly rigid walls. In this context, it is assumed that they are still valid in case of walls made of a real material from empirical considerations made in some of our previous works [48], as long as there is a strong impedance mismatch between the cavity fluid and the wall material itself.

From Eq. 1, the resonant response of the system is determined by geometrical parameters that are easy to estimate for S_{neck} and V_{cavity}. The effective neck length l_{eff} needs more considerations. In Ref. [48], a semi-analytical approach to estimate the length correction for a HR tuning frequency was proposed, and based on the fact that Rayleigh's formula [49] provides accurate for low ξ values (ξ is defined as the ratio between the representative lengths in the section plane of the neck and the cavity, respectively labeled as d_{neck} and d_{cavity}). It was empirically verified [48] that the effective length depends on the squared value of the ratio ξ. When the section area dimension of the neck is comparable with the section area dimension of the cavity ($\xi = 1$), the geometry and the obtained resonance frequency corresponds to a quarter-wavelength tube (QWT) and the previous relation is no more applicable.

2.2. Sound Transmission Loss

This work is focused on the evaluation of Sound Transmission Loss (TL) for the tested configurations. For a plane wave configuration at normal incidence ($\theta = \phi = 0°$, where θ and θ are the incidence angles around y and x axes, respectively), and thus oriented towards the negative direction of z axis (as illustrated in Figure 1), the TL is computed as defined in Eq. 2

$$\mathrm{TL} = 10\ \log_{10}\frac{\Pi_{incident}}{\Pi_{transmitted}}, \tag{2}$$

where $\Pi_{incident}$ and $\Pi_{transmitted}$ are the incident and transmitted sound powers, respectively. TL is the classical frequency indicator used to evaluate

the attenuation brought by a structure in terms of decibels as a function of frequency.

2.3. Transfer Matrix Method

The TL values related to the homogeneous and the meta-core models are all estimated through a Finite Element (FE) implementation of Eq. 2, see Section 2.2. The homogeneous results are also compared with those obtained with the AcuH toolbox of WaveTool [47]. This toolbox is used to perform a TMM-based TL calculation, by generalizing Eq. 3 and Eq. 4 for multi-layered configurations:

$$\mathrm{TL} = 10\,\log_{10}\left(\frac{1}{4}|T_{11} + \frac{T_{12}}{\rho_0 c_0} + \rho_0 c_0 T_{21} + T_{22}|^2\right), \tag{3}$$

$$\begin{bmatrix} T_{11} & T_{12} \\ T_{21} & T_{22} \end{bmatrix} = \begin{bmatrix} \cos(kd) & \mathrm{j}\sin(kd)Z_c \\ \frac{\mathrm{j}\sin(kd)}{Z_c} & \cos(kd) \end{bmatrix}, \tag{4}$$

with ρ_0 and c_0 being the density of air and the sound speed in air, respectively, while k is the wave number, d is the thickness, j is the imaginary unit and Z_c is the characteristic impedance.

2.4. Finite Elements calculations

The module "Pressure Acoustics and Frequency Domain" of COMSOL MultiPhysics is used both as modeling environment and numerical solver. For all structures presented in this work, the mesh consists of tetrahedral elements, generated through physics-controlled algorithms that are pre-implemented in the software. Considering that the recommended number of finite elements per wavelength depends on the degree of the shape functions, for the models discussed herein it is determined a minimum number of six elements per wavelength (Table 1), as recommended by Mace and Manconi [50] and recognized as a rule of thumb to ensure a reliable analysis. A Perfectly Matched Layer (PML) boundary condition is applied on the lowest face of the models. This represents an artificial absorbing layer for wave equations, commonly used to truncate computational regions in numerical methods in order to simulate problems with open boundaries (i.e. absorb outgoing waves from the interior of a computational region without reflecting them back). On the contrary, boundary conditions applied on faces normal to x- and y- axes are represented by classical Floquet-Bloch periodic conditions (see Figure 1 for axes definition).

Configuration	Domain elem.	Boundary elem.	Edge elem.
1	22212	6516	540
2	24434	7658	826
3	24531	7830	892
4	30019	8596	1014

Table 1: Number of FE mesh elements for each of the studied configurations.

3. Definition of the problem

In this work, several configurations are analyzed, whose properties are reported in Table 2. Some examples of the studied packages are shown in Figure 1; for the sake of clarity, a zoom on the inclusion of Configuration 4 is shown in Figure 2, to better highlight the presence of the neck on its upper side, which makes it a Helmholtz resonator.

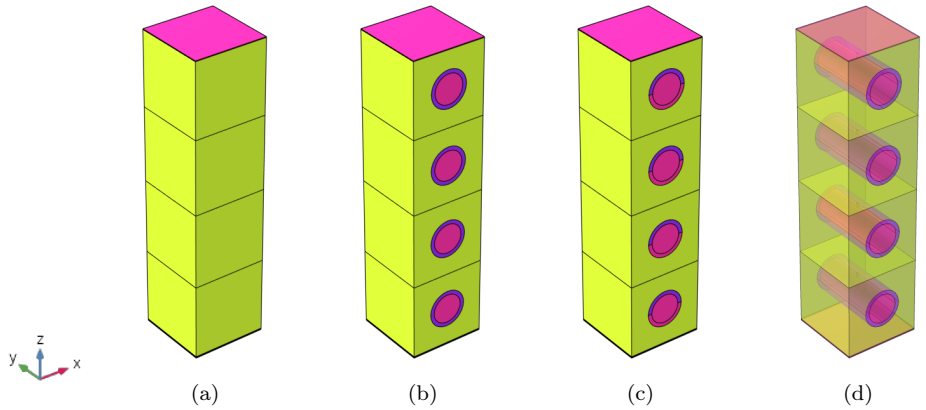


Figure 1: (a) Homogeneous acoustic package; (b) Hollow inclusions; (c) Half-cut hollow inclusions; (d) Helmholtz resonators.

3.1. Material and geometrical properties

The melamine layer is modeled as an equivalent fluid through the Johnson-Champoux-Allard approach [51, 52]. The FE implementation and analysis of this kind of materials has already been validated by the authors in their previous works [14], as well as for more complicated bi-phasic behaviors through the use of Biot theory of poro-elasticity [53]. The dimension d of the 3-dimensional cubic unit cell is 38 mm, while the outer radius r and the thickness t of the inclusions are respectively equal to 9.5 mm and 2 mm. Since

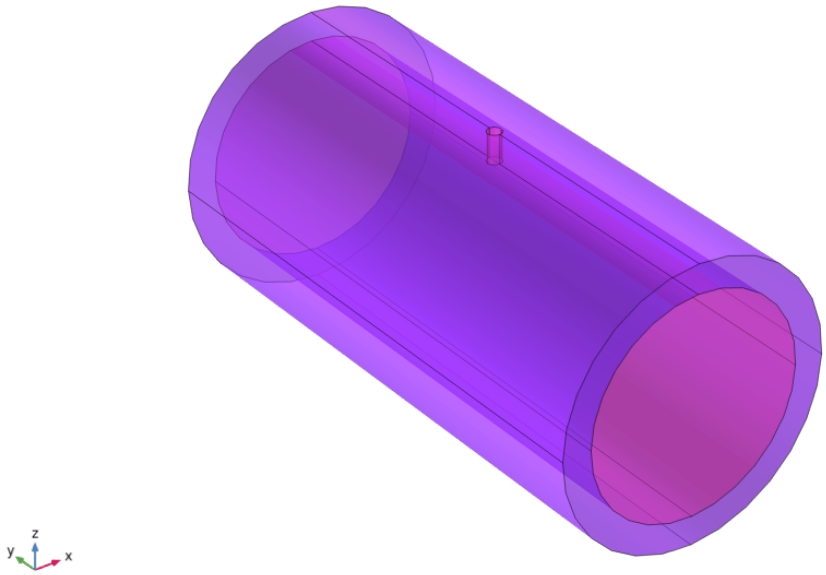


Figure 2: Zoom on the inclusion of Configuration 4, to highlight the presence of the Helmholtz resonator's neck.

the unit cells are repeated four times along the thickness, which has already been proved to be a sufficient number to exploit periodicity effects [54], the total thickness of the studied packages is $T = 152$ mm (the number of unit cell repetition is arbitrary and functional to the analysis). The geometrical and physical properties of the studied foam are reported in Table 3, while those related to the inclusions are reported in Table 4.

The aforementioned quantities are graphically explained in Figure 3. In summary:

- Configuration 1 represents the reference sequence of unit cells, made of homogeneous melamine (Figure 1(a)).
- Configuration 2 is meant to study the effect in terms of TL due to the insertion of a periodic pattern of hollow inclusions along the thickness (meaning that the repetition occurs on the z-direction as represented in Figure 1(b)), which leads to the excitation of an additional acoustic mode, and thus to a resonance peak; the adoption of hollow inclusions is

Configuration	Description
1	4 porous cells
2	4 porous cells with hollow inclusions
3	4 porous cells with hollow half-inclusions
4	4 porous cells with Helmholtz Resonators

Table 2: Description of the studied configurations.

Color	Yellow
Material	Melamine
Thickness [mm]	152
Porosity	0.99
Tortuosity	1
Airflow resistivity [Pa·s/m^2]	900
Viscous characteristic length [mm]	0.1
Thermal characteristic length [mm]	0.3

Table 3: Properties of JCA-modeled melamine.

made in order to improve efficiency in terms of mass control compared with the usage of plain inclusions.

- Configuration 3 is nearly similar to the previous one, but half-cut hollow inclusions are now used, as represented in Figure 1(c). The main objective of this design is to keep similar performances to that of Configuration 2, while further reducing weight (see Section 5).

- Configuration 4 starts from Configuration 2 and involves Helmholtz resonators made of aluminum into an acoustic package made of commonly-used melamine (Figure 1(d)). Each Helmholtz resonator is constituted by a hollow cylinder, with a hole acting as the neck, as shown in Figure 4.

In order to ease their manufacturing, inclusions have been made of aluminum but other materials could help reaching an optimal specific stiffness (i.e., the ratio between the stiffness and mass density properties), such as balsa wood that was considered in [54].
Properties of air (indicated with pink-colored layers) are: density $\rho_0 = 1.213[\frac{\mathrm{kg}}{\mathrm{m}^3}]$, speed of sound $c_0 = 342[\frac{\mathrm{m}}{\mathrm{s}}]$.

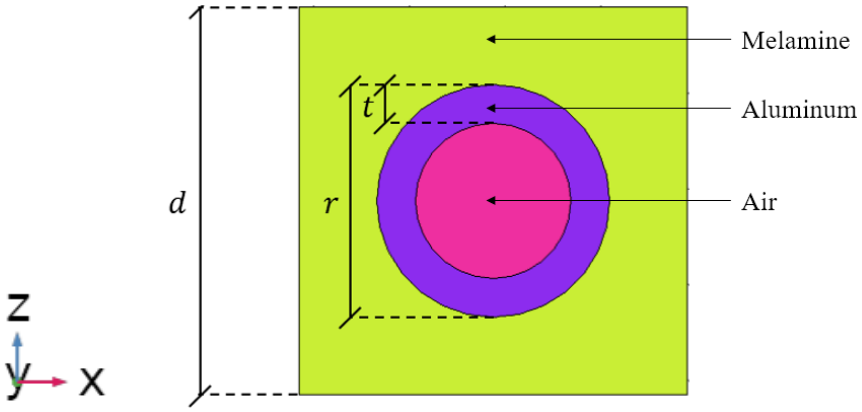


Figure 3: 2D view of a unit hollow inclusion, with graphical explanations of r, t and d

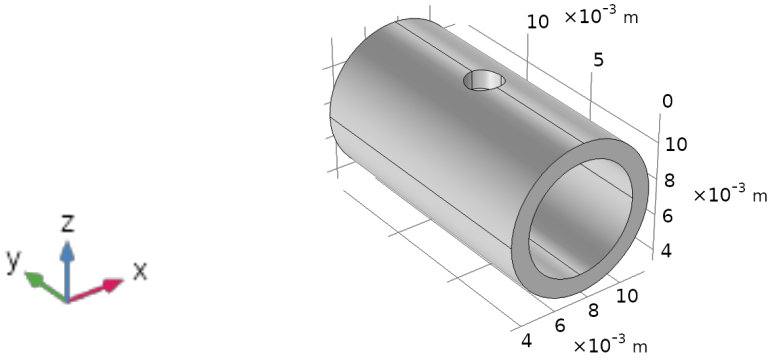


Figure 4: Geometry of the considered Helmholtz resonator [55].

Color	Purple
Material	Aluminum
Thickness [mm]	2
ρ **[kg/m^3]**	2700
E **[Pa]**	70 E+9
ν	0.33

Table 4: Properties of aluminum inclusions.

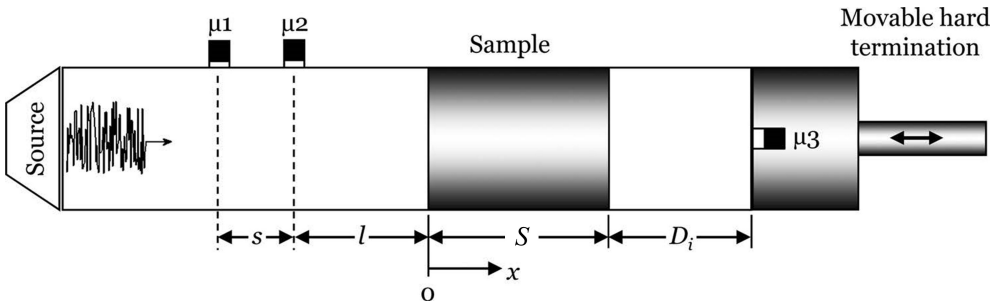


Figure 5: A sketch of an impedance tube configuration for three microphones, describing the incident and reflected wave and the positions of the microphones, speaker and sample [57].

4. Experimental comparisons and validation

A square impedance tube, equipped with three microphones, and a digital frequency analysis system are used for the measurement of normal incidence TL and acoustical properties of materials by determination of the sample's acoustic transfer matrix. The experimental facility and equipment have been provided by Mecanum Inc. [56]. A schematic representation of the experimental setup is shown in Figure 5. The square impedance tube has a constant rectangular cross-section with side-length of 38 mm, two microphones (μ_1 and μ_2) are mounted between the loudspeaker (source) and the sample, with a distance s between microphones of 25 mm and a distance l between the microphone μ_2 and the sample of 89 mm; the third microphone is mounted on the hard termination. Downstream the sample, an air cavity is added, whose thickness is adjusted with the movable hard termination. The distance s between microphones and the cross-section size dictate the measurements range of frequency, that is 400-4300Hz.

The three-microphone measurement method was originally developed by

Iwase *et al.* [58]. The version used in this work was developed by Salissou *et al.* [57] and relies on a 3 microphone 2 loads (3M2L) impedance tube method, an update of 4 microphone 2 loads (4M2L) method to optimize the number of measurements [57]. Two air cavities of fixed dimension $D_1 = 154.7$ mm and $D_2 = 172$ mm are used as loads for the 3M2L method. For any specimen, the transfer matrix T for the two cavity configurations is written according to ASTM E2611-09 in terms of the sound pressure p and particle velocity u on both faces of the sample (at $x = 0$ and $x = S$), and reported here:

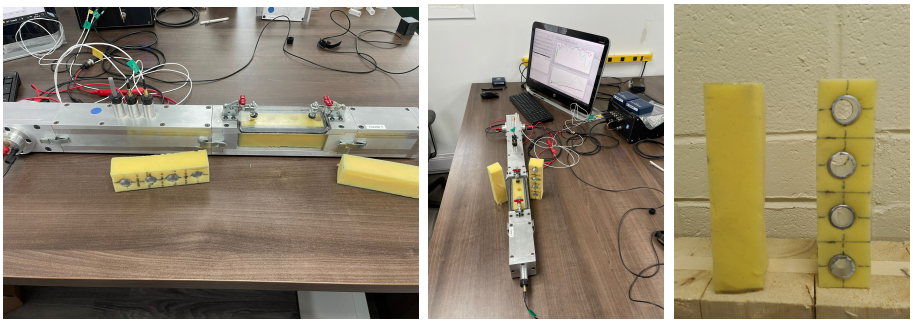
$$\mathbf{T} = \frac{1}{p_{1,S}u_{2,S} - p_{2,S}u_{1,S}} \begin{bmatrix} p_{1,0}u_{2,S} - p_{2,0}u_{1,S} & p_{2,0}p_{1,S} - p_{1,0}p_{2,S} \\ u_{1,0}u_{2,S} - u_{2,0}u_{1,S} & p_{1,S}u_{2,0} - p_{2,S}u_{1,0} \end{bmatrix}, \tag{5}$$

with $p_{i,0}$,$u_{i,0}$, $p_{i,S}$,$u_{i,S}$ that can be written as:

$$\begin{aligned} p_{i,0} &= -2je^{jkl}\frac{H_{12}\left(D_i\right)\sin(k(l+s)) - \sin(kl)}{H_{12}\left(D_i\right)e^{-jks} - 1}, \\ p_{i,S} &= -2je^{jkl}\frac{H_{13}\left(D_i\right)\sin(ks)\cos\left(kD_i\right)}{H_{12}\left(D_i\right)e^{-jks} - 1}, \\ u_{i,0} &= \frac{2e^{jkl}}{Z_S}\frac{H_{12}\left(D_i\right)\cos(k(l+s)) - \cos(kl)}{H_{12}\left(D_i\right)e^{-jks} - 1}, \\ u_{i,S} &= \frac{2e^{jkl}}{Z_S}\frac{H_{13}\left(D_i\right)\sin(ks)\sin\left(kD_i\right)}{H_{12}\left(D_i\right)e^{-jks} - 1}, \end{aligned} \tag{6}$$

with $H_{12}(D_i) = p_i(\mu_2)/p_i(\mu_1)$ transfer function between microphones 2 and 1 with air thickness D_i $(i = 1, 2)$, and $H_{13}(D_i) = p_i(\mu_3)/p_i(\mu_1)$ transfer function between microphones 3 and 1 with air thickness D_i, and Z_S and k respectively the specific acoustic impedance and the wave number of the air in the impedance tube. With all the coefficients and elements of the transfer matrix determined, the sound transmission loss is calculated as expressed by Eq. 3. Figure 6 shows the experimental setup, together with the melamine sample, that have been used in order to test Configurations 1 and 2, whose detailed geometrical and material description is reported in Tables 2, 3, 4 and 1.

As it can be appreciated from Figures 7 and 8, in the case of Configuration 1, analytical (TMM), numerical (FEM) and experimental results are in good agreement, with only some small oscillations in experimental data at mid-low frequencies. Concerning Configuration 2, the experimental tests show a broad peak brought by periodicity peak. This is attributed to the fact that



(a) (b) (c)

Figure 6: Experimental setup view from the tube side (a) and along its axis (b); tested samples (c).

actual damping of the sample is smaller than the one estimated by COMSOL MultiPhysics. Indeed, for equivalent fluid models, the damping coefficient is not directly defined by the user, but an "equivalent" quantity is estimated from the imaginary parts of density and bulk modulus.

5. Numerical analyses, results and discussion

The obtained results in terms of TL are presented in Figure 9, and Insertion Loss (IL) is also calculated in Figure 10 as the difference between the examined TL (Configurations 2-4) and that related to its homogeneous counterpart (Configuration 1) to better highlighted possible improvements. As expected, Configurations 2-4 show periodicity effects that result in increased TL values in a specific frequency range of frequencies, when half of the acoustic wavelength λ is equal to periodicity dimension d. Since this kind of acoustic resonance still relates on the thickness of the unit cell, it may be challenging to obtain performance peaks at low frequencies, when only a limited thickness is available. The proposed approach may conceptually be scaled also for low-frequency applications, but only when the total available thickness is sufficiently high, or if it is not considered as a model constraint (generally, both conditions are not applicable to solutions in the field of transport engineering). To improve TL at low frequency, a possible solution is to turn hollow inclusions into Helmholtz resonators (Configuration 4). As it can be noticed from the comparison plots reported in Figure 9 and Figure 10, the TL peak related to the Helmholtz resonance is narrower than the one generated by periodicity effects, but easier to tune at lower

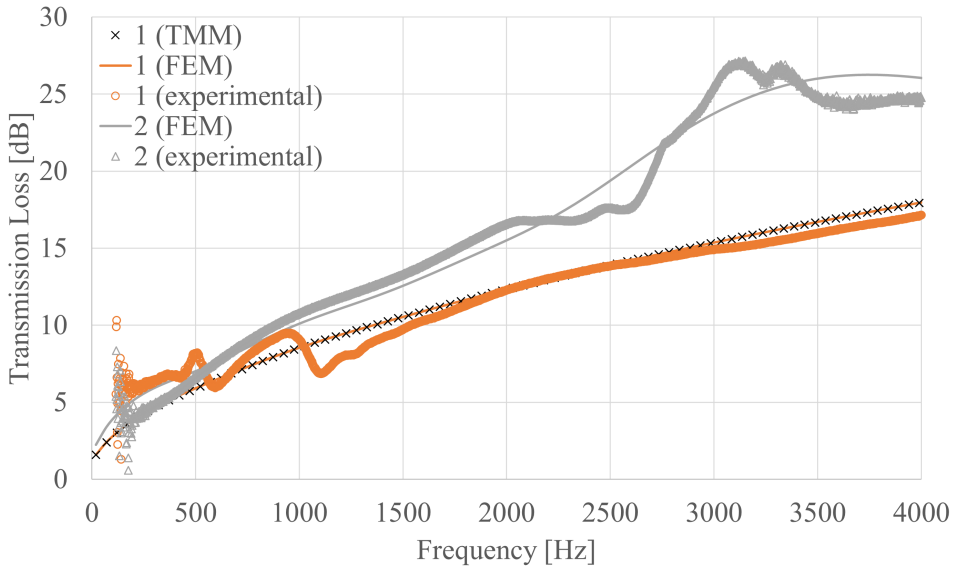


Figure 7: Transmission Loss of Configurations 1 and 2.

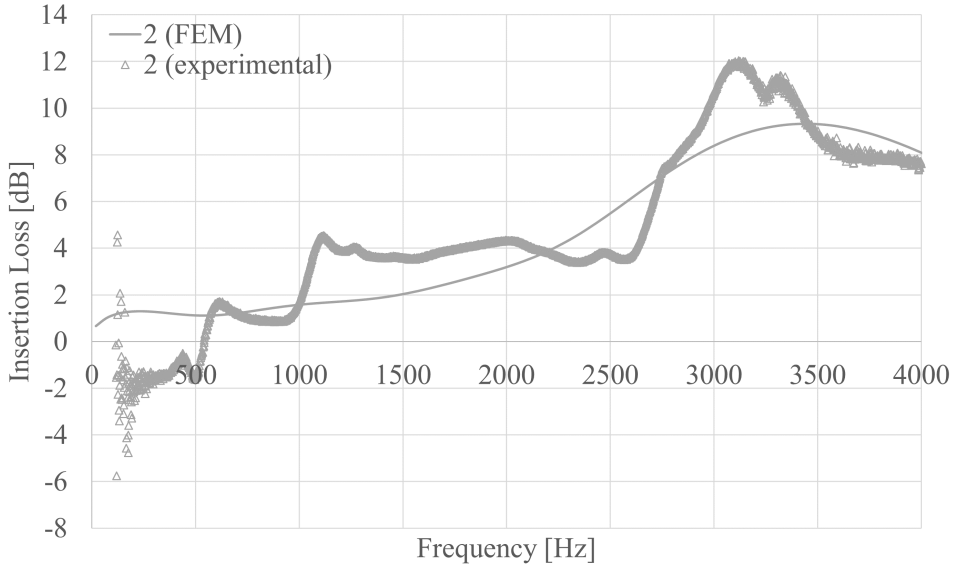


Figure 8: Insertion Loss of Configuration 2, with Configuration 1 as a reference

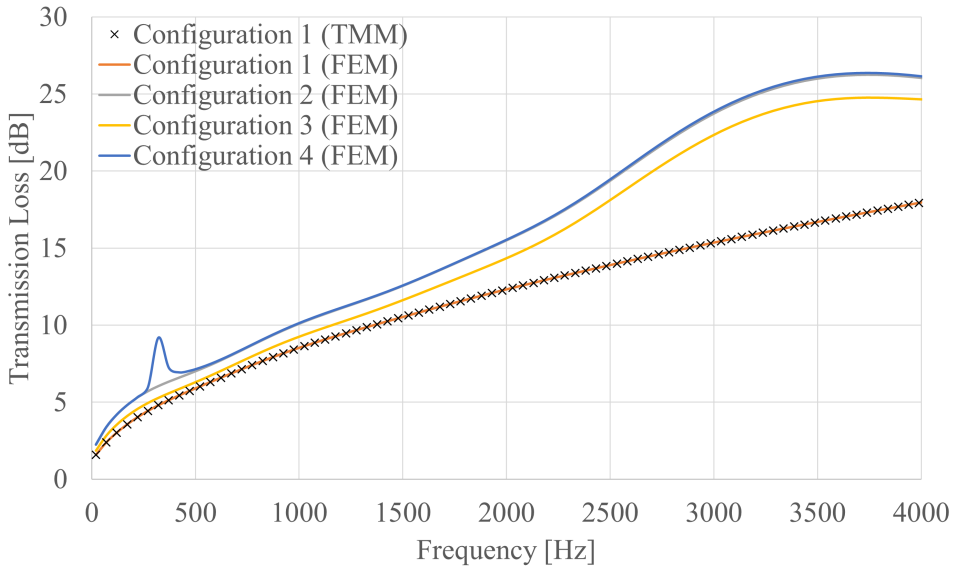


Figure 9: Transmission Loss of Configurations from 1 to 4 (TMM and FEM results).

frequency.

As it may be noted both Figure 9, the FE-based TL results related to the model having homogeneous layers show an almost perfect agreement with those analytically computed through the TMM. This comparison plays the role of an analytical validation of numerical results related to the multi-layered configuration without inclusions. It is not possible to directly perform the same kind of validation for the meta-configurations, since it is not conceptually possible to apply an analytical approach, such as the TMM, for non-homogeneous layers of material.

As shown in Figure 11, in Configuration 2 the hollow cylindrical inclusions lead to a maximum increase of TL peak amplitude of about 57% compared to Configuration 1. This result is further enhanced in Configuration 3, since it leads to a TL peak amplitude maximum increase of about 48%, but with a more limited increase in terms of mass due to the adoption of half-inclusions. Furthermore, in Configuration 4, the Helmholtz resonance phenomenon allows to reach a maximum increase of the TL peak amplitude of about 91%.

Moreover, the opportunity to introduce this class of meta-solutions for a realistic aeronautic application has already been considered in one of the authors' previous works [54], among other relevant studies that may be found

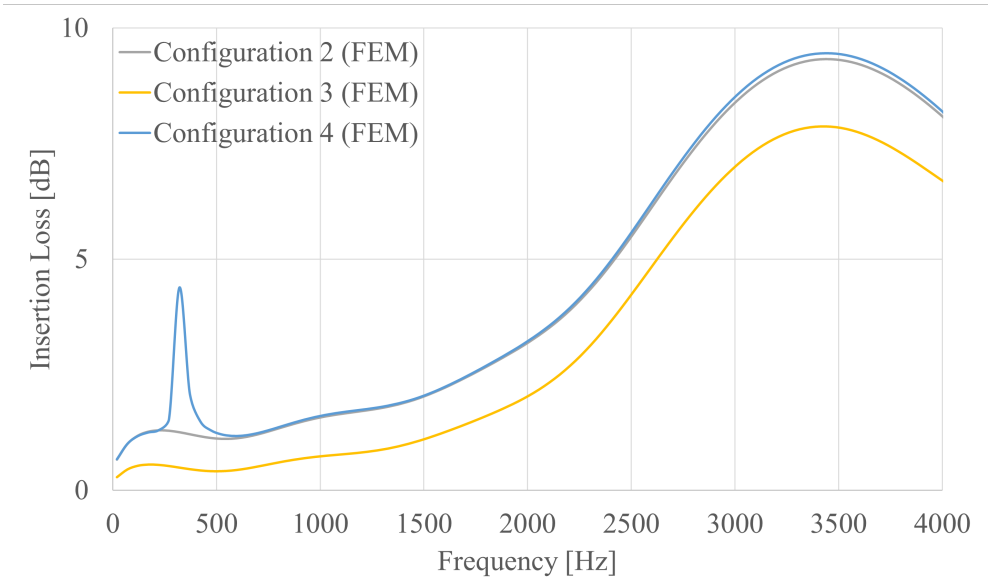


Figure 10: Insertion Loss of Configurations from 2 to 4, with Configuration 1 as a reference.

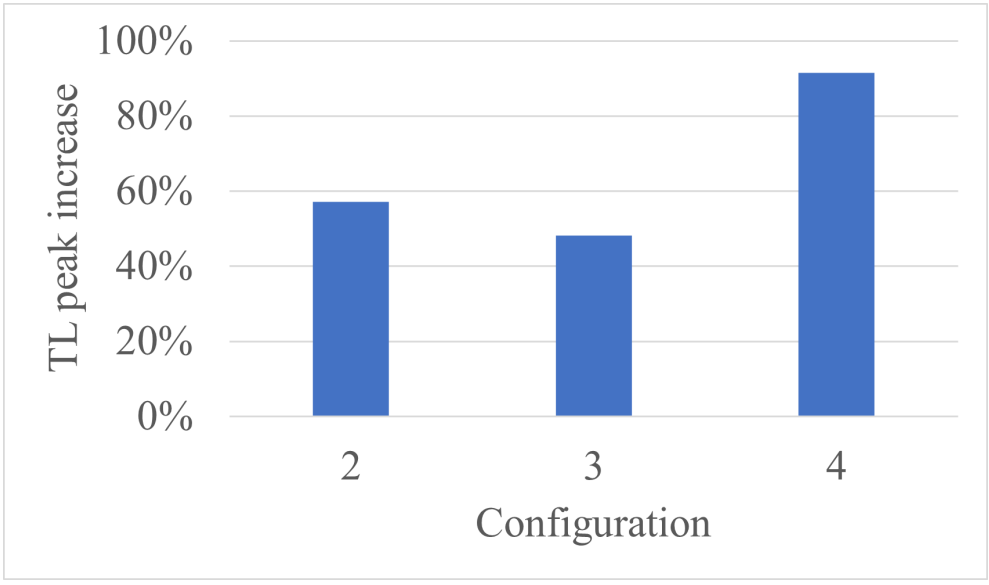


Figure 11: TL peak increments expressed in the form of bar charts, where Configuration 1 is considered as reference.

in literature [59–61]. In this context, it should be pointed out that HRs and periodic inclusions can theoretically greatly improve acoustic conditions in the cabin; indeed, although the TL may already seem high without the adoption meta-materials, a sound-emitting device such as an aircraft engine is particularly noisy and therefore conventional solutions may not be enough.

6. Parametric study for different incidence angles

The calculated TLs as a function of incidence angle, in the case of Configuration 4, are plotted in Figure 12, including all possible combinations of the cases with $\theta = 0°$, $\theta = 30°$, $\theta = 60°$, and $\phi = 0°$, $\phi = 30°$, $\phi = 60°$. The addition of periodic inclusions inside a homogeneous package can increase TL when the half-wavelength is almost equal to the length of periodicity. For any incidence angle combinations, both the periodic and the Helmholtz resonances still appear, even if they lead to different levels of response due to the fact that the fraction of the acoustics plane wave that is influenced by periodicity depends on incidence angle (for normal incidence, it is maximum). It can be noted that the effects of two generic θ_i and ϕ_j are the same of those related to θ_j and ϕ_i.

7. Conclusions

The main scope of the present research work is to propose solutions based on the inclusion of a periodic pattern inside a porous material, aiming at passively improving its acoustic performance in terms of sound transmissions loss, also considering the possibility to improve a standard aeronautical fuselage configuration by the insertion of this innovative package for enhancing noise suppression. In detail, a set of optimized configurations are numerically and experimentally studied, starting from the state of the art regarding the acoustic packages based on porous meta-materials. The main novelties of the present work are represented by the experimental validation of the acoustic meta-materials already studied in the previous works, together with the inclusion of a periodic pattern of Helmholtz resonators inside the foam core, aiming at passively improving its acoustic performance in an additional range of frequencies; furthermore, numerical results presented herein are also evaluated for different angles of incidence of the plane wave exciting the system. In order to reach this goal, some configurations are experimentally

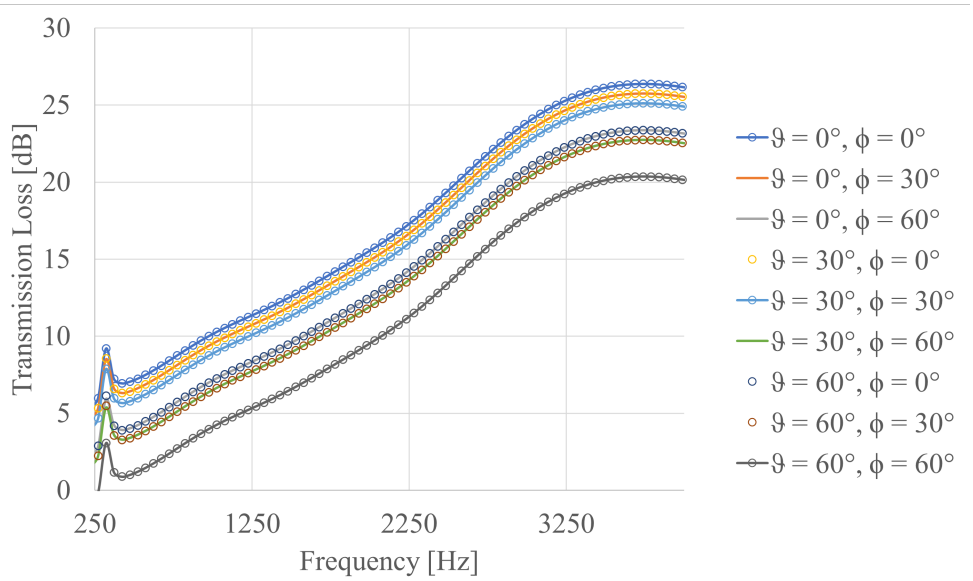


Figure 12: Transmission Loss of Configuration 4 with different angles of plane wave incidence.

analyzed, leading to a comparison and validation of the obtained numerical results. Subsequently, the effect of several periodic patterns (involving hollow cylindrical inclusions, half-cut hollow cylindrical inclusions and cylindrical Helmholtz resonators) are simulated; more specifically, numerical results are evaluated for different angles of incidence of the plane wave exciting the system. For each of these layouts, the associated mid-band amplitude of the Sound Transmission Loss peak, which is caused by the additional acoustic modes excited by the periodic nature of the meta-core itself, is estimated. Results obtained herein are presented in terms of tables and graphs, which may represent an unprecedented basis in order to pave the way for an optimized tunable and scalable sound-insulating acoustic package based on periodic porous meta-materials. Future works could focus on the analysis of more complex excitation loads. Most of all, it would be fundamental to investigate a way to reduce the mass increase related to the use of meta-cores, thus making this solution viable also for applications in transportation engineering and increasing its overall resource efficiency.

Acknowledgments

The authors acknowledge the support of the Italian Ministry of Education, University and Research (MIUR) through the project DEVISU, funded under the scheme PRIN-2017 - grant agreement No. 22017ZX9X4K006. Frédéric La Madeleine, Bachelor Student and Intern at "Centre de Recherche Acoustique-Signal-Humain, Department of Mechanical Engineering, Université de Sherbrooke" provided support to setup the samples.

References

[1] L. Cao, Q. Fu, Y. Si, B. Ding, J. Yu, Porous materials for sound absorption, Composite Communications 10 (2018) 25–35. doi:10.1016/j.coco.2018.05.001.

[2] X. D. Zhao, Y. J. Yu, Y. J. Wu, Improving low-frequency sound absorption of micro-perforated panel absorbers by using mechanical impedance plate combined with Helmholtz resonators, Applied Acoustics 114 (2016) 92–98. doi:10.1016/j.apacoust.2016.07.013.

[3] F. Yildiz, A. G. Parlar, Z. Parlar, M. Bakkal, Properties of sound panels made from recycled footwear treads, Acta Physica Polonica A 132 (3) (2017) 936–940. doi:10.12693/APhysPolA.132.936.

[4] P. K. Tang, W. A. Sirignano, Theory of a generalized helmholtz resonator, Journal of Sound and Vibration 26 (2) (1973) 247–262.

[5] C. Cai, C. M. Mak, Noise attenuation capacity of a Helmholtz resonator, Advanced Engineering Softwares 116 (2018) 60–66. doi:10.1016/j.advengsoft.2017.12.003.

[6] C. Lagarrigue, J. . Groby, O. Dazel, V. Tournat, Design of metaporous supercells by genetic algorithm for absorption optimization on a wide frequency band, Applied Acoustics 102 (2016) 49–54.

[7] L. Lv, J. Bi, C. Wei, X. Wang, Y. Cui, H. Liu, Effect of micro-slit plate structure on the sound absorption properties of discarded corn cob husk fiber, Fibers and Polymers 16 (7) (2015) 1562–1567. doi:10.1007/s12221-015-5002-x.

[8] U. Berardi, G. Iannace, Acoustic characterization of natural fibers for sound absorption applications, Building Environments 94 (2015) 840–852. doi:10.1016/j.buildenv.2015.05.029.

[9] X. Xinzhao, L. Guoming, L. Dongyan, S. Guoxin, Y. Rui, Electrically conductive graphene-coated polyurethane foam and its epoxy composites, Composite Communications 7 (2018) 1–6. doi:10.1016/j.coco.2017.11.003.

[10] J.-P. Groby, C. Lagarrigue, B. Brouard, O. Dazel, V. Tournat, Using simple shape three-dimensional inclusions to enhance porous layer absorption, Journal of Acoustical Society of America 136 (3) (2014) 1139–1148. doi:10.1121/1.4892760.

[11] Y. Yang, B. R. Mace, M. J. Kingan, Wave and finite element method for predicting sound transmission through finite multi-layered structures with fluid layers, Computers and Structures 204 (2018) 20–30. doi:10.1016/j.compstruc.2018.04.003.

[12] T. Weisser, Acoustic behavior of a rigidly backed poroelastic layer with periodic resonant inclusions by a multiple scattering approach, Journal of Acoustical Society of America 139 (2) (2016) 617–629. doi:10.1121/1.4940669.

[13] M. Gaborit, O. Dazel, P. Göransson, A simplified model for thin acoustic screens, Journal of Acoustical Society of America 144 (1) (2018) 76–81. doi:10.1121/1.5047929.

[14] D. Magliacano, S. Ahsani, M. Ouisse, E. Deckers, G. Petrone, W. Desmet, S. De Rosa, Formulation and validation of the shift cell technique for acoustic applications of poro-elastic materials described by the Biot theory, Mechanical Systems and Signal Processing 147 (2021). doi:10.1016/j.ymssp.2020.107089.

[15] Y. Cheng, C. Zhou, B. G. Yuan, D. J. Wu, Q. Wei, X. J. Liu, Ultra-sparse metasurface for high reflection of low-frequency sound based on artificial mie resonances, Nature Materials 14 (10) (2015) 1013–1019.

[16] M. Cinefra, G. D'Amico, A. De Miguel, M. Filippi, A. Pagani, E. Carrera, Efficient numerical evaluation of transmission loss in homogenized

acoustic metamaterials for aeronautical application, Applied Acoustics 164 (2020). doi:10.1016/j.apacoust.2020.107253.

[17] M. Moruzzi, M. Cinefra, S. Bagassi, Vibroacoustic analysis of an innovative windowless cabin with metamaterial trim panels in regional turboprops, Mechanics of Advanced Materials and Structures 28 (2) (2019) 1–13. doi:10.1080/15376494.2019.1682729.

[18] A. Casaburo, D. Magliacano, G. Petrone, F. Franco, S. De Rosa, Optimizing the acoustic properties of a meta-material using machine learning techniques, in: Proceedings of INTER-NOISE 2021 - 2021 International Congress and Exposition of Noise Control Engineering, 2021.

[19] A. Casaburo, D. Magliacano, G. Petrone, F. Franco, S. De Rosa, Gaussian-based machine learning algorithm for the design and characterization of a porous meta-material for acoustic applications, Applied Sciences (Switzerland) 12 (1) (2022).

[20] M. P. Thompson, H. W. Engleman, The two types of resonance in intake tuning, American Society of Mechanical Engineers, 1969.

[21] M. Driels, Dynamics of i. c. engine induction systems, Journal of Sound and Vibration 43 (3) (1975) 499–510. doi:10.1016/0022-460X(75)90003-6.

[22] R. T. Jameson, P. A. Hodgins, Improvement of the torque characteristics of a small, high-speed engine through the design of Helmholtz-tuned manifolding, SAE International (1990). doi:10.4271/900680.

[23] S. Mekid, M. Farooqui, Design of Helmholtz resonators in one and two degrees of freedom for noise attenuation in pipe lines, Acoustics Australia 40 (2012) 194–202.

[24] L. Gorny, G. Kooopmann, W. Neise, O. Lemke, Attenuation of Ducted Axial Propulsors' Blade Tone Noise Using Adaptively Tunable Resonators. doi:10.2514/6.2007-3529.

[25] D. Zhao, A. Morgans, Tuned passive control of combustion instabilities using multiple Helmholtz resonators, Journal of Sound and Vibration 320 (2009) 744–757. doi:10.1016/j.jsv.2008.09.006.

[26] J.-P. Groby, A. Wirgin, L. De Ryck, W. Lauriks, R. P. Gilbert, Y. S. Xu, Acoustic response of a rigid-frame porous medium plate with a periodic set of inclusions, Journal of Acoustical Society of America 126 (2) (2009) 685–693. doi:10.1121/1.3158936.

[27] L. Xiong, B. Nennig, Y. Aurégan, W. Bi, Sound attenuation optimization using metaporous materials tuned on exceptional points, Journal of Acoustical Society of America 142 (4) (2017) 2288–2297. doi:10.1121/1.5007851.

[28] Y. Tang, S. Ren, H. Meng, F. Xin, L. Huang, T. Chen, C. Zhang, T. J. Lu, Hybrid acoustic metamaterial as super absorber for broadband low-frequency sound, Sci Rep 259 (2017). doi:10.1038/srep43340.

[29] R. Talebitooti, H. D. Gohari, Optimization of sound transmission through composite cylinder with poroelastic core considering vcm, Mechanics of Advanced Materials and Structures 27 (3) (2020) 238–249. doi:10.1080/15376494.2018.1472345.

[30] B. Wang, T. Dou, A quasi-3d layer-wise finite element model for vibroacoustic analysis of finite sandwich plates with frequency-dependent viscoelastic core, Mechanics of Advanced Materials and Structures (2022). doi:10.1080/15376494.2022.2095064.

[31] R. Vaicaitis, M. Slazak, Noise transmission through stiffened panels, Journal of Sound and Vibration 70 (3) (1980) 413–426. doi:10.1016/0022-460X(80)90309-0.

[32] X. Li, K. Yu, Vibration and acoustic responses of composite and sandwich panels under thermal environment, Composite Structures 131 (2015) 1040–1049. doi:10.1016/j.compstruct.2015.06.037.

[33] Y. Yang, B. Li, Z. Chen, N. Sui, Z. Chen, M.-U. Saeed, Y. Li, R. Fu, C. Wu, Y. Jing, Acoustic properties of glass fiber assembly-filled honeycomb sandwich panels, Composites Part B: Engineering 96 (2016) 281–286. doi:10.1016/j.compositesb.2016.04.046.

[34] F. X. Xin, T. J. Lu, Sound radiation of orthogonally rib-stiffened sandwich structures with cavity absorption, Composites Science and Technology 70 (15) (2010) 2198–2206. doi:10.1016/j.compscitech.2010.09.001.

[35] F. X. Xin, T. J. Lu, Analytical modeling of wave propagation in orthogonally rib-stiffened sandwich structures: Sound radiation, Computers and Structures 89 (5-6) (2011) 507–516. doi:10.1016/j.compstruc.2010.12.007.

[36] M. P. Arunkumar, J. Pitchaimani, K. V. Gangadharan, M. C. Lenin Babu, Influence of nature of core on vibro acoustic behavior of sandwich aerospace structures, Aerospace Science and Technology 56 (2016) 155–167. doi:10.1016/j.ast.2016.07.009.

[37] M. P. Arunkumar, M. Jagadeesh, J. Pitchaimani, K. V. Gangadharan, M. C. L. Babu, Sound radiation and transmission loss characteristics of a honeycomb sandwich panel with composite facings: Effect of inherent material damping, Journal of Sound and Vibration 383 (2016) 221–232. doi:10.1016/j.jsv.2016.07.028.

[38] F. X. Xin, T. J. Lu, Effects of core topology on sound insulation performance of lightweight all-metallic sandwich panels, Materials and Manufacturing Processes 26 (9) (2011) 1213–1221. doi:10.1080/10426914.2010.531241.

[39] G. L. Ghiringhelli, M. Terraneo, E. Vigoni, Improvement of structures vibroacoustics by widespread embodiment of viscoelastic materials, Aerospace Science and Technology 28 (1) (2013) 227–241. doi:10.1016/j.ast.2012.11.003.

[40] T.-C. Hung, J.-S. Huang, Y.-W. Wang, K.-Y. Lin, Inorganic polymeric foam as a sound absorbing and insulating material, Construction and Building Materials 50 (2014) 328–334. doi:10.1016/j.conbuildmat.2013.09.042.

[41] J. Zhou, A. Bhaskar, X. Zhang, Sound transmission through a double-panel construction lined with poroelastic material in the presence of mean flow, Journal of Sound and Vibration 332 (16) (2013) 3724–3734. doi:10.1016/j.jsv.2013.02.020.

[42] J. Zhou, A. Bhaskar, X. Zhang, The effect of external mean flow on sound transmission through double-walled cylindrical shells lined with poroelastic material, Journal of Sound and Vibration 333 (7) (2014) 1972–1990. doi:10.1016/j.jsv.2013.11.038.

[43] Y. Liu, Sound transmission through triple-panel structures lined with poroelastic materials, Journal of Sound and Vibration 339 (2015) 376–395. doi:10.1016/j.jsv.2014.11.014.

[44] W. Larbi, J. F. Deü, R. Ohayon, Vibroacoustic analysis of double-wall sandwich panels with viscoelastic core, Computers and Structures 174 (2016) 92–103. doi:10.1016/j.compstruc.2015.09.012.

[45] Y. Liu, C. Daudin, Analytical modelling of sound transmission through finite clamped double-wall sandwich panels lined with poroelastic materials, Composite Structures 172 (2017) 359–373. doi:10.1016/j.compstruct.2017.03.024.

[46] D. Griese, J. D. Summers, L. Thompson, The effect of honeycomb core geometry on the sound transmission performance of sandwich panels, Journal of Vibration and Acoustics, Transactions of the ASME 137 (2) (2015). doi:10.1115/1.4029043.

[47] Waveset - engineering innovation.
URL https://wavesetconsulting.com

[48] G. Catapane, D. Magliacano, G. Petrone, A. Casaburo, F. Franco, S. De Rosa, Semi-analytical estimation of Helmholtz resonators' tuning frequency for scalable neck-cavity geometric couplings, CEAS Aeronautical Journal (2022).

[49] J. W. S. Rayleigh, The Theory of Sound, Cambridge University Press, 1898.

[50] B. R. Mace, E. Manconi, Modelling wave propagation in two-dimensional structures using finite element analysis, Journal of Sound and Vibration 318 (2008) 884–902. doi:10.1016/j.jsv.2008.04.039.

[51] D. L. Johnson, J. Koplik, R. Dashen, Theory of dynamic permeability and tortuosity in fluid-saturated porous media, Journal of Fluid Mechanics 176 (1) (1987) 379–402. doi:10.1017/S0022112087000727.

[52] Y. Champoux, J. F. Allard, Dynamic tortuosity and bulk modulus in air-saturated porous media, Journal of Applied Physics 70 (4) (1991) 1975–1979. doi:10.1063/1.349482.

[53] M. Biot, Mechanics of deformation and acoustic propagation in porous media, Journal of Applied Physiscs 33 (4) (1962) 1482–1498. doi:10.1063/1.1728759.

[54] D. Magliacano, G. Petrone, F. Franco, S. De Rosa, Numerical investigations about the sound transmission loss of a fuselage panel section with embedded periodic foams, Applied Acoustics 182 (2021). doi:10.1016/j.apacoust.2021.108265.

[55] G. Catapane, D. Magliacano, G. Petrone, F. Franco, S. De Rosa, Periodic resonator-based optimization of an acoustic package made of glass wool, in: Resource Efficient Vehicle Conference, 2021.

[56] M. Inc., Acoustic experts.
URL https://www.mecanum.com/en

[57] Y. Salissou, R. Panneton, O. Doutres, Complement to standard method for measuring normal incidence sound transmission loss with three microphones, Journal of the Acoustical Society of America 131 (3) (2012) EL216–EL222.

[58] T. Iwase, Y. Izumi, R. Kawabata, A new measuring method for sound propagation constant by using sound tube without any air spaces back of a test material, in: INTER-NOISE and NOISE-CON congress and conference proceedings, Vol. 1998, Institute of Noise Control Engineering, 1998, pp. 1265–1268.

[59] M. C. Moruzzi, M. Cinefra, S. Bagassi, Vibroacoustic analysis of an innovative windowless cabin with metamaterial trim panels in regional turboprops, Mechanics of Advanced Materials and Structures 28 (14) (2021) 1509–1521. doi:10.1080/15376494.2019.1682729.

[60] B. Balakrishnan, A. Rajagopal, S. Raja, Vibroacoustic performance assessment of aircraft panels in low, mid and high frequency regimes, Mechanics of Advanced Materials and Structures 29 (20) (2022) 2942–2961. doi:10.1080/15376494.2021.1882015.

[61] H. Kaidouchi, S. Kebdani, S. A. Slimane, Vibro-acoustic analysis of the sound transmission through aerospace composite structures, Mechanics of Advanced Materials and Structures (2022). doi:10.1080/15376494.2022.2085348.

List of Tables

1 Number of FE mesh elements for each of the studied configurations. 8
2 Description of the studied configurations. 10
3 Properties of JCA-modeled melamine. 10
4 Properties of aluminum inclusions. 12

List of Figures

1 (a) Homogeneous acoustic package; (b) Hollow inclusions; (c) Half-cut hollow inclusions; (d) Helmholtz resonators. 8
2 Zoom on the inclusion of Configuration 4, to highlight the presence of the Helmholtz resonator's neck. 9
3 2D view of a unit hollow inclusion, with graphical explanations of r, t and d 11
4 Geometry of the considered Helmholtz resonator [55]. 11
5 A sketch of an impedance tube configuration for three microphones, describing the incident and reflected wave and the positions of the microphones, speaker and sample [57]. 12
6 Experimental setup view from the tube side (a) and along its axis (b); tested samples (c). 14
7 Transmission Loss of Configurations 1 and 2. 15
8 Insertion Loss of Configuration 2, with Configuration 1 as a reference 15
9 Transmission Loss of Configurations from 1 to 4 (TMM and FEM results). 16
10 Insertion Loss of Configurations from 2 to 4, with Configuration 1 as a reference. 17
11 TL peak increments expressed in the form of bar charts, where Configuration 1 is considered as reference. 17
12 Transmission Loss of Configuration 4 with different angles of plane wave incidence. 19